EBioMedicine 45 (2019) 314–327

Contents lists available at ScienceDirect

EBioMedicine

journal homepage: www.ebiomedicine.com

EBioMedicine
Published by THE LANCET

Research paper

mTORC2/Akt activation in adipocytes is required for adipose tissue inflammation in tuberculosis

Nuria Martinez [a], Catherine Y. Cheng [b], Natkunam Ketheesan [a,c], Aidan Cullen [a], Yuefeng Tang [d], Josephine Lum [b], Kim West [a], Michael Poidinger [b], David A. Guertin [d], Amit Singhal [b,e,f], Hardy Kornfeld [a,*]

[a] Department of Medicine, University of Massachusetts Medical School, Worcester, MA, USA
[b] Singapore Immunology Network, Agency for Science, Technology and Research (A*STAR), Singapore
[c] School of Science and Technology, University of New England, Australia
[d] Department of Molecular Medicine, University of Massachusetts Medical School, Worcester, MA, USA
[e] Lee Kong Chian School of Medicine, Nanyang Technological University, Singapore
[f] Vaccine and Infectious Disease Research Centre (VIDRC), Translational Health Science and Technology Institute (THSTI), Faridabad, Haryana, India

ARTICLE INFO

Article history:
Received 27 March 2019
Received in revised form 26 June 2019
Accepted 27 June 2019
Available online 4 July 2019

Keywords:
Tuberculosis
Adipose tissue
Inflammation
mTORC2
Akt
Insulin resistance

ABSTRACT

Background: Mycobacterium tuberculosis has co-evolved with the human host, adapting to exploit the immune system for persistence and transmission. While immunity to tuberculosis (TB) has been intensively studied in the lung and lymphoid system, little is known about the participation of adipose tissues and non-immune cells in the host-pathogen interaction during this systemic disease.
Methods: C57BL/6J mice were aerosol infected with *M. tuberculosis* Erdman and presence of the bacteria and the fitness of the white and brown adipose tissues, liver and skeletal muscle were studied compared to uninfected mice.
Findings: M. tuberculosis infection in mice stimulated immune cell infiltration in visceral, and brown adipose tissue. Despite the absence of detectable bacterial dissemination to fat tissues, adipocytes produced localized pro-inflammatory signals that disrupted adipocyte lipid metabolism, resulting in adipocyte hypertrophy. Paradoxically, this resulted in increased insulin sensitivity and systemic glucose tolerance. Adipose tissue inflammation and enhanced glucose tolerance also developed in obese mice after aerosol *M. tuberculosis* infection. We found that infection induced adipose tissue Akt signaling, while inhibition of the Akt activator mTORC2 in adipocytes reversed TB-associated adipose tissue inflammation and cell hypertrophy.
Interpretation: Our study reveals a systemic response to aerosol *M. tuberculosis* infection that regulates adipose tissue lipid homeostasis through mTORC2/Akt signaling in adipocytes. Adipose tissue inflammation in TB is not simply a passive infiltration with leukocytes but requires the mechanistic participation of adipocyte signals.

1. Introduction

Tuberculosis (TB) remains the leading cause of death by infectious diseases worldwide. According to the World Health Organization, an estimated 1.6 million people died from *M. tuberculosis* infection in 2017 [1]. Lacking an environmental reservoir, *M. tuberculosis* has adapted to the human host over some 70,000 years of coevolution [2] to ensure its perpetuation that depends on low host mortality and immune pathology that enables aerosol transmission. The bacillus may persist in a lifelong latent state in ~90% of infected individuals and when active TB develops, the average duration of untreated disease prior to death or non-sterilizing recovery is estimated to be 2–3 years [3]. The chronicity of TB compared to most acute infectious diseases imposes unique and incompletely understood systemic effects in the host-pathogen interaction. Alveolar macrophages are the first host cells infected with inhaled *M. tuberculosis*, but dissemination is universal even in clinical latency [4]. Upon recognition of the bacteria, alveolar macrophages induce the release of chemokines that initiates the migration of secondary myeloid cells like dendritic cells and neutrophils to the lung [5]. These cells engulf and disseminate the bacteria to lymphoid tissues where T cells are primed at around 9–10 days in mice and after exposure to the pathogen [6]. Antigen specific T cells are

* Corresponding author.
E-mail address: Hardy.Kornfeld@umassmed.edu (H. Kornfeld).

https://doi.org/10.1016/j.ebiom.2019.06.052

Research in context

Evidence before the study

Tuberculosis (TB) is a chronic infectious disease that mainly affects the lungs, but advanced TB is marked by cachexia that was historically called consumption. Previous studies identified bacterial dissemination to liver and, with high dose infection, to adipose tissues but the impact of TB disease on the metabolic function of those organs has not been investigated.

Added value of this study

Modeling *M. tuberculosis* infection in mice, we found that TB was associated with increased systemic glucose tolerance and insulin signaling in adipocytes. Surprisingly, the infection promoted adipocyte hypertrophy and adipose tissue inflammation, which are typically associated with insulin resistance. Mice on a high fat diet had higher adipose tissue inflammation after infection, but better glucose tolerance than the uninfected mice. Adipose tissue inflammation depended on mTORC2/Akt signaling in adipocytes, revealing a previously unknown role for adipocytes in the host response to TB.

Implications of all the available evidence

This study uncovers a paradoxical metabolic adaptation of the host in TB. We provide insight on the mechanistic signaling that causes adipose tissue inflammation and glucose and lipid metabolism dysregulation during TB and possible targets for therapeutic intervention.

found in the lung as early as 18–20 days after infection, at a point where macrophages are activated, and the bacterial growth plateaus. Common sites for disseminated TB include lymphoid tissues, bones, the gastrointestinal tract, and pleura, but virtually any tissue may be targeted including adipose tissue [7,8]. Presence of the bacteria in adipocytes has been shown in vitro and in adipose tissue biopsies from TB patients [9–11]. In mice, bacteria were found in visceral adipose tissue after infection with higher aerosol doses (~200 CFU) or different routes of infection (intravenously at 8×10^4 CFU and intranasal at 320 CFU) [10–12].

The adipose tissue is an endocrine organ that communicates with other organs to regulate systemic metabolic fitness [13]. Adipose tissue has also been implicated in immunity, participating in a signaling network that involves the endothelium, lungs, and bone marrow [14]. It has been well described that *M. tuberculosis* modifies the lipid and glucose metabolism at a cellular level, by differentiating macrophages into foamy cells [15] and by triggering switch from oxidative phosphorylation to glycolytic metabolism in lung T cells and macrophages [16], but any organ and systemic metabolic regulation are completely unknown. Here, we report increased leukocyte infiltration and cytokine expression in adipose tissues of lean mice and mice fed a high fat diet (HFD) following low-dose aerosol infection with *M. tuberculosis*. This inflammatory response occurred without detectable bacteria in adipose tissues, it was followed by adipocyte hypertrophy, and it was paradoxically associated with increased systemic glucose tolerance. This response was associated with increased adipose tissue Akt S473 phosphorylation, while adipocyte-specific depletion of the mTOR complex 2 (mTORC2) subunit Rictor, which is essential for Akt S473 phosphorylation, abrogated adipose tissue inflammation, cytokine expression, and adipocyte hypertrophy in mice with TB. Our data suggest an alternative to the classical metaflammation model by showing that *M. tuberculosis* infection uncouples adipose tissue inflammation and adipocyte hypertrophy from increased lipolysis, insulin resistance, and glucose intolerance. These results demonstrate a novel host-pathogen interaction linking immunity and metabolism in TB.

2. Materials and methods

2.1. Mice

Age matched (6–8 wk. old) male C57BL/6J mice were obtained from Jackson Laboratory (Bar Harbor, ME) and Adiponectin-Cre;Rictor$^{fl/fl}$ mice were supplied by Dr. Guertin (UMMS). Mice were housed in the Animal Medicine facility at UMMS where experiments were performed under protocols approved by the Institutional Animal Care and Use Committee and Institutional Biosafety Committee.

Mice were aerosol infected with *M. tuberculosis* Erdman using a Glas-Col Inhalation Exposure System (Terre Haute, IN) set to deliver ~50 CFU to the lung. Mice were fed a HFD (60% fat content, isocaloric) (Research Diets, New Brunswick, NJ). Mice were weighed weekly, blood glucose measurements were performed with a BD Logic glucometer (Becton Dickinson, Franklin Lakes, NJ) biweekly and blood samples and tissues were taken after 2, 4, 8 and 20 weeks of infection.

2.2. Pre-adipocyte isolation and differentiation

Stromal vascular fraction (SVF) cells were isolated from the inguinal white adipose tissue (iWAT) as previously described and using a gentleMACS Dissociator (Miltenyi Biotec Inc., Auburn, CA) with collagenase [17]. Cells were seeded in 48 well plates and infected with *M. tuberculosis Erdman* at a MOI10 for 24, 48 or 72 h. Gene expression of cytokines by quantitative PCR and cell volume using a Beckman Coulter Z2 cell counter (Beckman Coulter Life Sciences, Indianapolis, IN) were measured in these cells.

2.3. Flow cytometry

Cells were isolated from the tissues and stained with Zombie Aqua Viability Kit and for CD45 APC-Cy7, CD3 PE-Cy7, CD64 PE-594, CD11c PE, CD11b PercP-Cy5.5, Ly6C A700, Ly6G FITC and MHC-II Bv421 (Biolegend, San Diego, CA). Other staining panels were used: CD3 PercPCy5.5, CD8 FITC, CD4 PE, CD40L PE-Cy7 and CD69 A700. Data was acquired on an LSR-II (BD Biosciences, San Jose, CA) and analyzed with FlowJo v10. Gating strategy is detailed in Supplementary Figs. S1A and S2.

2.4. Quantitative PCR

Zymo RNA extraction kit (Zymo Research Corp, Irvine, CA) was used to isolate total RNA from tissue or cells. Equal amounts of RNA were retro-transcribed with High Capacity Reverse Transcription Kit (Applied Biosystems). Real-time PCR for *Ccl2*, *Ccl5*, *Cxcl1*, *Cxcl2*, *Il1b*, *Tnfa*, *Il6*, *Il4*, *Il10*, *Il13*, *Lpl*, *Cd36*, *Pnpla2, Lipe, Cebpa, Ppara, Pparg, Bmp4 and Ebf1* was performed at 60 °C of annealing temperature and using Applied Biosystems SYBR Green PCR mix. *Tpb,Gapdh* and *ActB* were used as housekeeping genes and primer sequences were designed by Primer3 input (Supplementary Table S1). Results were calculated as fold change to the control group by the delta-delta Ct method.

2.5. Bacterial growth

Whole tissue was homogenized in PBS containing 0.05% Tween 80 and cells from the SVF fraction were lysed in 10% Triton X-100. Homogenates were plated on 7H11 agar plates and colonies were counted after 3 weeks.

2.6. M. tuberculosis chromosome equivalent quantitative PCR

Bacterial genomic DNA was extracted and the qPCR for SigF DNA fragment was performed following the protocol from Munoz-Elias et al. [18]. Briefly, mycobacterial genomic DNA was extracted after homogenizing the tissue and using phenol-chloroform-isoamyl alcohol solution (25:24:1) and several centrifugation steps. Quantitative PCR was performed using TaqMan Universal Master Mix II (Applied Biosystems).

2.7. RNAsequencing

RNA was isolated from tissue followed by a Qiagen RNeasy Micro clean-up procedure (Qiagen, Hilden, Germany) according to the manufacturer's protocol. RNAs were analyzed on Perkin Elmer Labchip GX system (Perkin Elmer, Waltham, MA, USA) for quality assessment with RNA Quality Score ≥ 7.9. cDNA libraries were prepared using 2 ng of total RNA and 1 μl of a 1:50,000 dilution of ERCC RNA Spike in Controls (Ambion® Thermo Fisher Scientific, Waltham, MA, USA) using SMARTSeq v2 protocol [19] except for the following modifications: 1. Use of 20 μM TSO, 2. Use of 250 pg of cDNA with 1/5 reaction of Illumina Nextera XT kit (Illumina, San Diego, CA, USA). The length distribution of the cDNA libraries was monitored using DNA High Sensitivity Reagent Kit on the Perkin Elmer Labchip. All samples were subjected to an indexed PE sequencing run of 2 × 51 cycles on an Illumina HiSeq 2000.

Reads were mapped to MM10 with STAR v2.2.3 and gencode M9 annotation. Gene counts were determined with feature counts, differential gene expression with edgeR in R v 3.1.2 [20]. Data analysis was performed in pipeline pilot (www.accelrys.com) and plots generated in Spotfire (www.tibco.com).

2.8. Morphological analysis

Images of the perigonadal white adipose tissue (pgWAT), iWAT and interscapular brown adipose tissue (iBAT) were taken on a bright field microscope at 4× magnification. Using ImageJ 1.46r (NIH, Bethesda, MD) cell area was quantified, for pgWAT and iWAT, and lipid droplet area, for iBAT in ~200 cells. Cells were distributed in different bins according to their size and percentage was calculated.

Area of lung lesion was measured in proportion to total lung area using ImageJ 1.46r.

2.9. Biochemical analysis

Glycerol (Sigma-Aldrich, St Louis, MO), NEFA (Cell Biolabs, Inc., San Diego, CA), insulin, adiponectin, leptin (R&D Systems, Minneapolis, MN), HDL, LDL and total cholesterol (Cell Biolabs) were analyzed in plasma or media following the manufacturer's guidelines. Triglycerides (TG) (Cayman Chemicals, Ann Arbor, MI) were measured in tissue homogenates from pgWAT, liver and quadriceps (quad).

2.10. Immunoblotting

Total protein was obtained from adipose tissue, quantified by BCA assay (Pierce Biotechnology, Rockford, IL) and SDS-PAGE separated. Antibodies rabbit anti-mouse for P-HSL, HSL, P-IR, IR, S473Akt, T408Akt, total Akt and β-actin (Cell signaling Technology Inc., Danvers, MA) were used and bands were quantified by ImageJ 1.46r.

2.11. Metabolic analysis

The insulin tolerance test (ITT) and glucose tolerance test (GTT) were performed after 6 h or overnight fasting, respectively. Mice were injected with 0·75 U/kg insulin for ITT or 1 mg/kg lucose for GTT and blood glucose was measured before and at several time points after injection.

2.12. Bone marrow transfer

Bone marrow cells were isolated from WT or KO mice and 10^6 cells were transferred via tail vein injection into lethally irradiated WT or KO mice. After 6–8 wk., mice were infected with *M. tuberculosis* Edrman by aerosol and tissues were harvested 4 or 8 wk. post infection (p.i.).

2.13. Statistical analysis

GraphPad Prism 6.0 was used to perform statistical analysis. When normality was confirmed, data were analyzed using a Student's *t*-test or by the Mann-Whitney *U* test if otherwise. A p value of $<0{\cdot}05$ was considered statistically significant.

2.14. Data and software availability

The data generated from the RNAsequencing (RNAseq) experiment can be found at: https://www.ncbi.nlm.nih.gov/geo/query/acc.cgi?acc=GSE106611

3. Results

3.1. Aerosol M. tuberculosis infection promotes adipose tissue inflammation

To investigate the involvement of the tissues linked to glucose and lipid metabolism and the progression towards insulin resistance [13,21] (adipose tissue, liver and skeletal muscle) in TB pathogenesis, we tracked tissue-associated leukocytes in lean C57BL/6J mice infected with 50 CFU of *M. tuberculosis* Erdman by aerosol. SVF cells isolated from pgWAT, iWAT, and iBAT at 2, 4, and 8 wk. p.i. were characterized by flow cytometry as follows: macrophages (MΦ; $CD11b^+CD11c^-$), inflammatory macrophages (IMΦ; $CD11c^+$), polymorphonuclear cells or neutrophils (PMN; $Ly6G^+$), dendritic cells (DC; $CD64^-CD11c^+$ $MHCII^+$) and $CD3^+$ T cells (gating strategy shown in Supplementary Fig. S1a). The number of total SVF cells and the number of IMΦ, DC and T cells were significantly increased in pgWAT at 4 wk. p.i. (Fig. 1a and Supplementary Fig. S1b) while all of them were increased at 8 wk. p.i. in both pgWAT and liver (Fig. 1a and Supplementary Fig. S1c). Only the number of MΦ, IMΦ and T cells were significantly increased in iBAT at 8 wk. p.i. and MΦ, PMN and T cells in quad at 8 wk. p.i. (Fig. 1c and Supplementary Fig. S1d). Just a few populations were significantly increased in iBAT (Fig. 1c), liver and quad (Supplementary Fig. S1c-d) at 4 wk. p.i. while iWAT did not show any differences at all the time points (Fig. 1b). These results demonstrate that low dose aerosol infection with virulent *M. tuberculosis* is associated with a generalized leukocyte inflammatory response occurring within weeks in visceral and brown adipose tissues and liver while only a few populations are increased in quadriceps.

Inflammation could result from proliferation of resident adipose tissue leukocytes and/or recruitment of immune cells from the circulation. To address this question, we used Ly6C surface marker that it is differentially expressed by patrolling monocytes which replenish the resident population ($Ly6C^-$) vs pro-inflammatory monocytes that are recruited to inflammatory environments ($Ly6C^+$) [22,23]. The number of MΦ and IMΦ that were $Ly6C^+$ was significantly higher in the pgWAT from infected mice at 8 wk. p.i. (Fig. 1d). Numbers of $Ly6C^-$ cells were also increased in the infected tissues, although to a lesser degree and not significantly (Fig. 1d), indicating that MΦ accumulation in pgWAT during TB results mainly from recruitment. Both numbers of $Ly6C^-$ and $Ly6C^+$ populations in IMΦ were increased in iBAT and liver, while quad only had $Ly6C^-$ cells increased in IMΦ (Supplementary Fig. S2a).

Adipose tissue inflammation in obesity has been proposed to be initiated by resident natural killer (NK) cell proliferation in response to cell stress and death of hypertrophic adipocytes [24,25]. This triggers recruitment of $CCR2^+$ (also $Ly6C^+$) monocytes and skewing of MΦ towards an M1 phenotype, which is associated with increased systemic

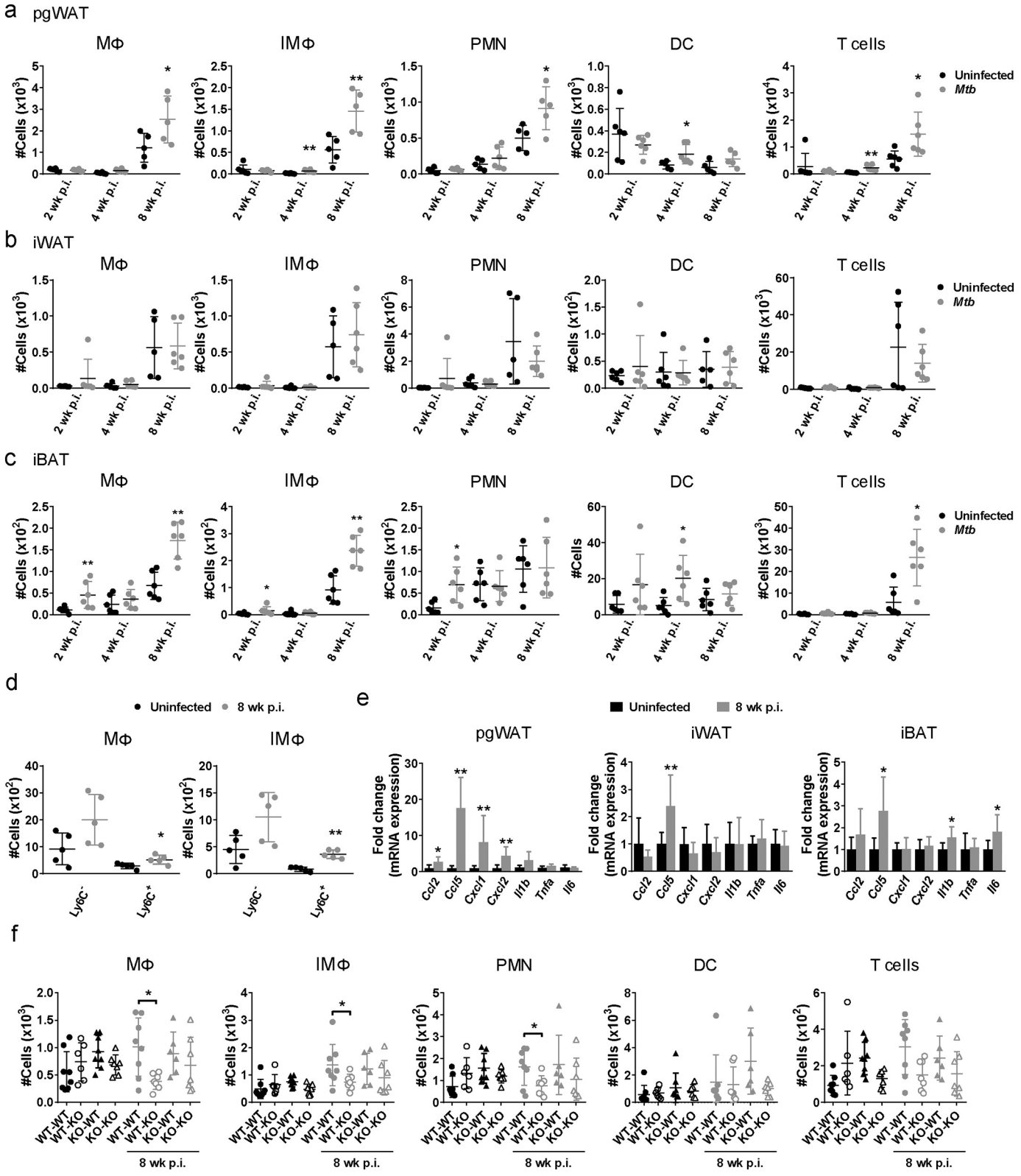

Fig. 1. Adipose tissue inflammation following aerosol *M. tuberculosis infection*. Number of macrophages (MΦ), inflammatory macrophages (IMΦ), polymorphonuclear cells (PMN), dendritic cells (DC) and T cells in perigonadal white adipose tissue (pgWAT) (a), inguinal white adipose tissue (b) and interscapular brown adipose tissue (c) from uninfected mice or mice infected for 2, 4 and 8 wk. (d) Number of Ly6C^{-} and Ly6C^{+} populations in MΦ and IMΦ from pgWAT from uninfected mice or mice infected for 8 wk. (e) Gene expression of *Ccl2*, *Ccl5*, *Cxcl1*, *Cxcl2*, *Il1b*, *Tnf1*, and *Il6* in pgWAT, iWAT and iBAT expressed as fold-change in tissues of infected vs uninfected mice 8 wk. after aerosol challenge. (f) Bone marrow cells from WT or TLR2/4 DKO mice were adoptively transferred to lethally irradiated WT or TLR2/4 DKO recipient mice. Number of MΦ, IMΦ, PMN, DC and T cells in pgWAT from uninfected mice or mice infected for 8 wk. Data are expressed as mean ± SD (n = 6–8). All experiments were repeated at least twice. *$P < 0{\cdot}05$ and **$P < 0{\cdot}01$. See also Supplementary Figs. S1 and S2.

insulin resistance. In the present study, the total number of NK1.1$^+$ cells isolated from pgWAT was not higher in *M. tuberculosis*-infected mice (Supplementary Fig. S2b). This suggests that adipose tissue inflammation in the setting of TB operates by pathways distinct from those responsible for non-infectious metaflammation.

We next compared tissue mRNA levels of selected cytokines in pgWAT, iWAT, iBAT, liver and quad of uninfected mice and in mice 2,4 and 8 wk. after *M. tuberculosis* challenge (Fig. 1e and S2c). Infected mice exhibited significant elevation of *Ccl2*, *Ccl5*, *Cxcl1* and *Cxcl2* mRNA in pgWAT at 8 wk. p.i. (Fig. 1e). Changes in *Ccl5* gene expression started early after infection, 4 wk., and *Il1b* and *Tnfa* gene expression were only increased at 4 wk. p.i. in pgWAT (Supplementary Fig. S2c). In general, cytokines were elevated in iWAT at 2 wk. p.i., but not at 4 and 8 wk., while most of the cytokines were increased in the liver at 4 and 8 wk. p.i. (Fig. 1e and Supplementary Fig. S2c). iBAT and quad had *Ccl5* elevated at 4 and 8 wk. p.i., although to a lesser degree than observed in pgWAT (Fig. 1e and Supplementary Fig. S2c). There was also a modest but statistically significant increase of *Il1b* and *Tnfa* gene expression in iBAT at 4 wk. p.i. and *IL1b* and *Il6* at 8 wk. p.i. We also measured the gene expression of the anti-inflammaroty cytokines *Il4*, *Il10* and *IL13*. *Il13* was not detected in any of the tissues and *Il4* and *Il10* were not significantly different in pgWAT, iWAT and iBAT between uninfected mice and 8 wk. p.i. (Supplementary Fig. S2c). While differing in intensity and time, an inflammatory response was observed in each of the three major types of adipose tissue. In pgWAT and liver changes in cytokine expression were coincident with increased number of inflammatory cells.

Liver is a well-recognized target for bacterial dissemination in the mouse TB model, but adipose tissue and skeletal muscle are uncommon sites for disseminated TB. To test if the inflammation in the adipose tissue was triggered by bacterial dissemination from the lung, we plated whole tissue and SVF fraction but unexpectedly failed to observe growth of *M. tuberculosis*. To assess whether non-replicating bacilli were sequestered in adipose tissue we quantified bacterial chromosome equivalents by qPCR [18] but no amplification of the sigF DNA fragment was detected (data not shown). Finally, using yellow fluorescent protein (YFP)-expressing *M. tuberculosis* Erdman by microscopy, we identified only two fields with possible single bacilli present whereas lung sections contained high numbers of fluorescent bacilli. Our inability to detect *M. tuberculosis* in pgWAT of infected mice suggested that adipose tissue inflammation in vivo was not primarily driven by bacterial dissemination to fat in contrast to the inflammation in lung and liver that harbor a high bacterial burden.

Since *M. tuberculosis* is known to release vesicles containing lipoproteins and glycolipids that stimulate macrophages in a TLR2-dependent manner [26] the presence of culturable bacteria is not necessarily required to provoke adipose tissue inflammation in TB. Adipocytes express TLR2 and TLR4 [27] and could therefore respond to cognate ligands associated with *M. tuberculosis*. To test if TLR2 and TLR4 signaling are activated in adipocytes during *M. tuberculosis* infection, we performed reciprocal adoptive transfer of syngeneic bone marrow into irradiated recipients using WT and TLR2/4 double KO mice (Fig. 1f). Irradiated TLR2/4 KO mice that received bone marrow from WT donors did not present an increased number of MΦ, IMΦ and PMN in pgWAT after 8 wk. of infection. Together, our data suggest that TLR2/4 signaling in non-hematopoietic cells, presumably adipocytes, was essential for the recruitment and proliferation of these populations of leukocytes in pgWAT during infection.

3.2. T cell activation in adipose tissue of infected mice

To further characterize the pathways that were activated in the pgWAT from *M. tuberculosis*-infected mice, we performed RNAseq in whole tissue at 8 wk. p.i. and compared the transcriptomic profiles to adipose tissues from uninfected mice. Genes associated with antigen presentation and Th1 and type-1 interferon responses, such as HLA-E, HLA-DQA1, B2M, CD74, STAT1, GBP4, and GBP6 were found to be upregulated in the pgWAT of infected mice (Fig. 2a and Supplementary Table S2). Ingenuity pathway analysis of differentially expressed genes confirmed these findings (Fig. 2b). Enhanced expression of chemokines including CCL8, CXCL9, CXCL10 and the receptor CXCR6 was also observed. This indicated the presence of activated T cells in pgWAT of infected mice that was confirmed by flow cytometry (Fig. 2c). We found an increased percentage of CD4$^+$ and CD8$^+$ T cells that were CD40L$^+$ and CD8$^+$ T cells expressing the early activation marker CD69 (Fig. 2c; gating strategy shown in Supplementary Fig. S3a). In mouse models of obesity (in the absence of infection) antigen-specific adipose-resident T cell become activated and this depends mainly on MHC class II expression by resident and recruited MΦ [28] and by other non-immune (CD45$^-$) cells [29]. In our TB model, upregulation of MHC-II expression was identified by RNAseq (Fig. 2a and Supplementary Table S2) and confirmed by flow cytometry on both MΦ and CD45$^-$-SVF cells (Fig. 2d-e). To test whether *M. tuberculosis*-antigen specific T cells were present in adipose tissue, we stained CD4$^+$ and CD8$^+$ SVF fraction T cells with TB10.4 and ESAT-6 tetramers. No TB10.4$^+$ or ESAT-6$^+$ T cells were identified in the pgWAT after 8 wk. of infection (Supplementary Fig. S3b). Together, these results demonstrate correlation between the number of MHC-II$^+$ cells and T cell activation, but this did not appear to be driven by a specific response to immunodominant *M. tuberculosis* antigens.

3.3. M. tuberculosis induces adipocyte cytokine production and hypertrophy

Whole adipose tissues are highly heterogeneous; thus, to evaluate the specific contribution of the mature adipocyte fraction to cytokine production, we infected differentiated primary adipocytes with *M. tuberculosis* in vitro (MOI 10, 24 h) and analyzed cytokine gene expression (Fig. 3a). Results showed a similar pattern as in whole tissue, including notably high expression of *Ccl5* with infection. This experiment, together with the analysis of the tissue inflammation in the adoptively transferred TLR2/4 double KO mice, reveal a positive link between aerosol *M. tuberculosis* infection and adipose tissue inflammation that was associated with the recruitment of immune cells and the stimulation of pro-inflammatory signals in the adipocytes themselves.

Visceral adipose tissue inflammation has been linked to progression from non-diabetic obesity to insulin resistance and ultimately to T2D [21,30]. This inflammation is believed to be initiated by adipocyte hypertrophy with associated cell stress and cell death [31]. To investigate whether *M. tuberculosis* infection provokes adipocyte hypertrophy we compared adipose tissue mass and adipocyte cell area in pgWAT and iWAT or the lipid droplet area in iBAT. Starting at 8 wk. p.i. adipocytes in pgWAT had significantly increased average cell size (2543 vs 1776 μm^2 in uninfected mice) along with increased percentage of hypertrophied cells (area > 5000 μm^2) and a corresponding reduced percentage of cells with small area (0–1200 μm^2) (Fig. 3b). A similar trend was observed in iWAT of infected mice, but no significance was found (Fig. 3c). The iBAT of infected mice had an increased lipid droplet area (722 vs 519 μm^2 in uninfected mice) along with a higher percentage of lipid droplets >1200 μm^2 and a lower percentage of lipid droplets ≤300 μm^2 (Fig. 3d). Taken together, these data indicate that pulmonary *M. tuberculosis* infection alters lipid storage in adipose tissues. One possible explanation for adipocyte hypertrophy without a corresponding increase in adipose tissue mass (Supplementary Fig. S4a) would be increased adipocyte cell death without a compensatory increase in adipogenesis. We also concluded that adipocyte hypertrophy was dependent on local inflammation by neighbor immune cells and/or long exposure to *M. tuberculosis*, as primary adipocytes in vitro did not increase cell volume after 24, 48 and 72 h of infection (MOI 10) (Supplementary Fig. S4b-c).

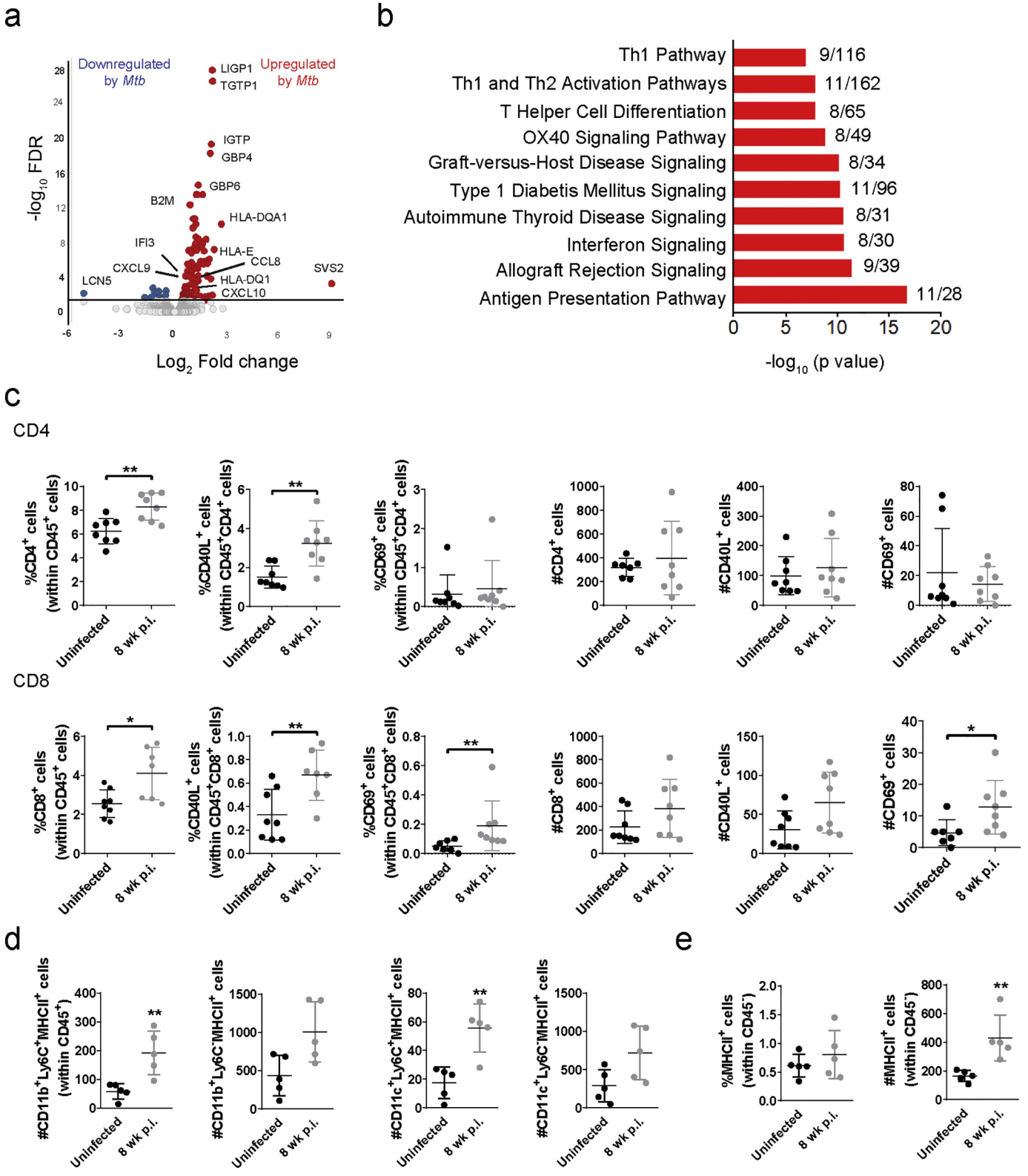

Fig. 2. *M. tuberculosis* infection induces T cell activation in white adipose tissue. (a) RNA from pgWAT of uninfected and infected mice at 8 wk. was used for RNAseq (Supplementary Table S2). Volcano plots depicting the $\log_2$ fold change between uninfected and infected versus the $-\log_{10}$ FDR. (b) Canonical pathways enrichment analysis of the 135 differentially expressed genes in Mtb infected adipose tissue using IPA. (c) Percentage and number of $CD4^+$ and $CD8^+$ T cells, $CD40L^+$ cells, and $CD69^+$ cells in pgWAT. (d) Number of MHC-II^+ cells in CD11b $^+$Ly6C$^-$, CD11b $^+$Ly6C$^-$, CD11c $^+$Ly6C$^-$ and CD11 $^+$Ly6C$^+$ in pgWAT. (e) Percentage and number of MHC-II^+ cells in $CD45^-$ cells. Data are expressed as mean ± SD (n = 6–8). Flow analysis experiments were repeated twice. *$P < 0{\cdot}05$ and **$P < 0{\cdot}01$. See also Supplementary Fig. S3.

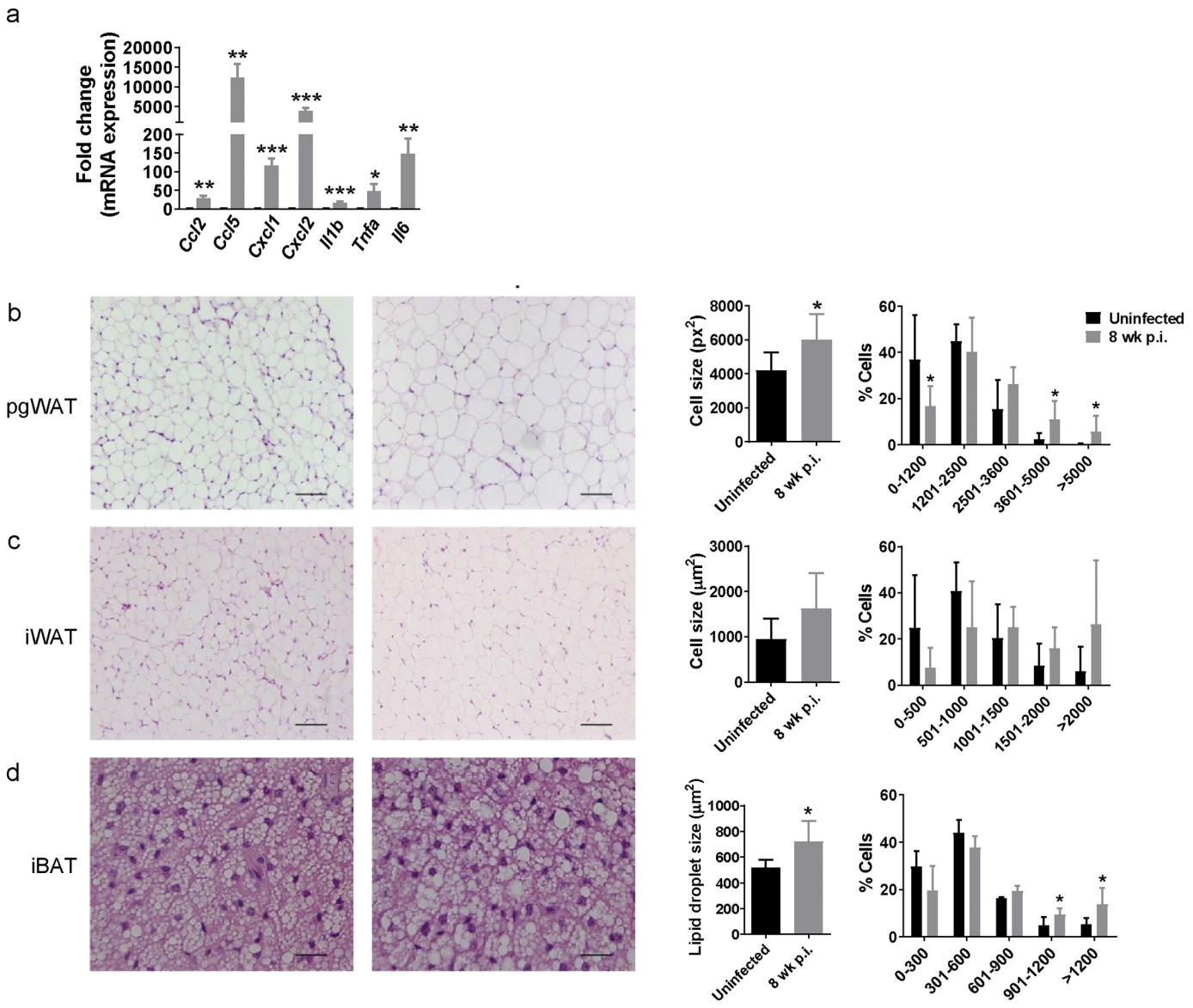

Fig. 3. *M. tuberculosis* infection induces adipocyte hypertrophy in white and brown adipose tissue. (a) Gene expression of *Ccl2*, *Ccl5*, *Cxcl1*, *Cxcl2*, *Il1b*, *Tnf1*, and *Il6* in primary differentiated adipocytes, expressed as fold-change, uninfected and infected in vitro at a MOI 10 for 24 h. Left, representative images of H&E staining from (b) perigonadal white adipose tissue (pgWAT), (c) inguinal white adipose tissue (iWAT), and (d) interscapular brown adipose tissue (iBAT) from uninfected mice or mice infected with *M. tuberculosis* for 8 wk. Scale bar is 100 µm. Middle, Mean of adipocyte area size from pgWAT and iWAT or lipid droplet area size from iBAT. Around 200 cells/mouse were quantified and averaged. Right, Percentage of cells/lipid droplet distributed in different bins regarding their area. Data are expressed as mean ± SD (n = 6). The experiment was repeated twice. *P < 0·05.

3.4. Adipose tissue lipid and glucose metabolism in M. tuberculosis-infected mice

Dietary composition and total food intake by chow-fed mice in our experiments were unchanged before or after aerosol challenge (Supplementary Fig. S4d). We therefore considered whether homeostatic lipid uptake and/or metabolism were altered in infected mice. Lipolysis is the predominant mechanism regulating fat storage and adipocyte cell size in response to signals induced by insulin, catecholamines, growth hormone, and TNF-α among others. The scavenger receptor CD36 and lipoprotein lipase (*Lpl*) also participate in fatty acid uptake and lipid storage in adipocytes [32,33]. There was a trend for lower expression of ATGL (*Pnpla2*) and HSL (*Lipe*), that catalyze lipolysis, and *Cd36* gene expression only in pgWAT of infected mice but this did not reach statistical significance, whereas expression of *Lpl* was significantly lower in infected mice (Fig. 4a).

We next measured plasma levels of glycerol and NEFA, products of lipolysis, in fasted mice that were infected or not with *M. tuberculosis* for 8 wk. and 15 min after i.p. injection of PBS or insulin, that inhibits lipolysis. While there was no difference between groups in plasma levels of glycerol or NEFA after PBS injection, the *M. tuberculosis*-infected mice had lower levels of glycerol and NEFA in plasma under insulin stimulation (Fig. 4b). Activation of lipolysis in adipose tissue was evaluated by quantifying HSL phosphorylation, which showed a non-significant decrease in pgWAT of insulin-stimulated, *M. tuberculosis*-infected mice (Fig. 4c). Taken together, although the tissue mass (Supplementary Fig. S4a) and concentration of TG in the adipose tissue (Supplementary Fig. S4e) do not change, these data suggest that *M. tuberculosis* further decreases lipolysis under insulin stimulation.

The effect of insulin to stimulate glucose uptake and modulate lipid metabolism is mediated by Akt [13]. In *M. tuberculosis*-infected mice, Akt S473 phosphorylation was significantly increased under fasting

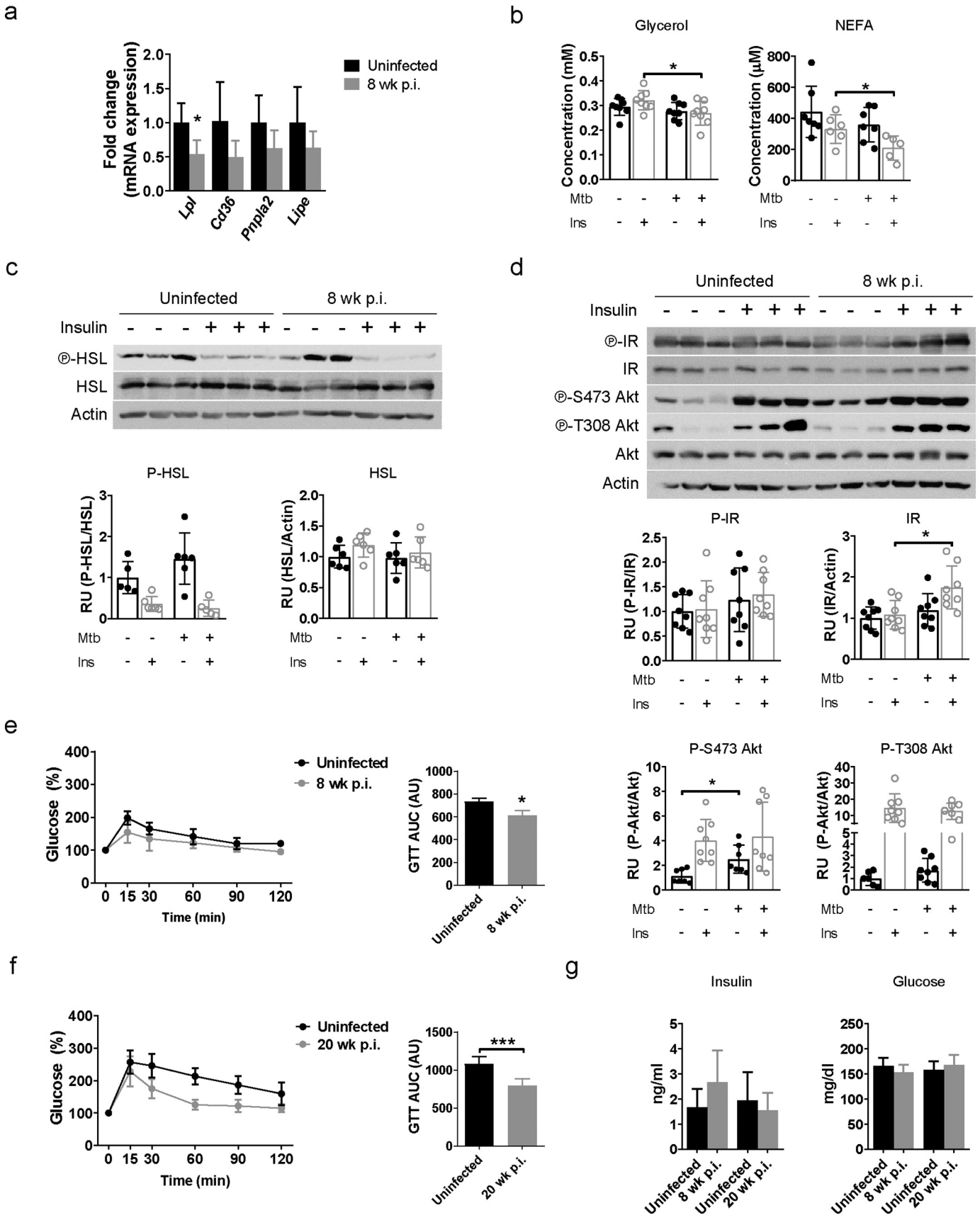
a
Fold change (mRNA expression)
Uninfected
8 wk p.i.
Lpl
Cd36
Pnpla2
Lipe
b
Glycerol
NEFA
Concentration (mM)
Concentration (μM)
Mtb
Ins
c
Uninfected
8 wk p.i.
Insulin
Ⓟ-HSL
HSL
Actin
P-HSL
HSL
RU (P-HSL/HSL)
RU (HSL/Actin)
d
Ⓟ-IR
IR
Ⓟ-S473 Akt
Ⓟ-T308 Akt
Akt
P-IR
IR
RU (P-IR/IR)
RU (IR/Actin)
e
Glucose (%)
Time (min)
Uninfected
8 wk p.i.
GTT AUC (AU)
P-S473 Akt
P-T308 Akt
RU (P-Akt/Akt)
f
20 wk p.i.
g
Insulin
Glucose
ng/ml
mg/dl

conditions at 8 wk. p.i. (Fig. 4d), but no further increase was observed when insulin-stimulated. Since S473 of Akt is a phosphorylation site for mTORC2, that regulates cellular metabolism, our results indicate that mTORC2 was activated in response to *M. tuberculosis* infection [34]. Insulin receptor expression was slightly and significantly increased during infection when mice were insulin treated (Fig. 4d) but to assess insulin-responsiveness at a systemic level we next performed ITT and GTT at different time points after infection. No significant difference in the ITT curves was observed in infected mice (Supplementary Fig. S4f). However, mice that were infected for 8 wk. (Fig. 4e) and for 20 wk. (Fig. 4f), were more glucose tolerant than uninfected mice. We concluded that under the conditions of these experiments and despite the development of adipose tissue inflammation, infection was associated with increased insulin sensitivity in adipocytes and systemic glucose tolerance. However, plasma insulin levels and fasted blood glucose were no different after 8 and 20 wk. of *M. tuberculosis* infection (Fig. 4g). Other markers linked to adipose tissue inflammation and obesity and T2D including plasma HDL, LDL, total cholesterol, and TG were also unchanged upon infection (Supplementary Fig. S4g–h).

In the liver, *Lpl* and *Lipe* gene expression was significantly increased but there was no difference in tissue TG content (Supplementary Fig. S5a-b). Also, there was no change in basal or insulin-stimulated phosphorylation of IR or Akt in liver from *M. tuberculosis*-infected mice (Supplementary Fig. S5c). Despite that adipocyte hypertrophy and associated inflammation are typically linked with insulin resistance [21], our data showed that mice with TB had paradoxically normal systemic glucose metabolism and increased Akt activation and adipocyte insulin response.

3.5. *M. tuberculosis* infection exacerbates HFD-induced adipose tissue inflammation

Mice with HFD-induced obesity have increased adipose tissue inflammation and develop disrupted lipid metabolism characterized by adipocyte hypertrophy and insulin resistance within a few weeks of starting diet [21]. To test whether *M. tuberculosis* infection would accelerate or otherwise alter that process, we placed mice on a HFD (60% fat content) for 8 wk. before aerosol challenge and then harvested tissues 8 wk. p.i. We confirmed that HFD upregulates inflammation in the pgWAT (Fig. 5a), iWAT and iBAT (data not shown) of uninfected mice and that *M. tuberculosis* infection further slightly exacerbated accumulation of IMΦ compared to the uninfected HFD mice. By 20 wk. p.i. there was no longer a difference in the leukocyte content of infected vs uninfected mice, perhaps reflecting progressive, age-related adipose tissue inflammation in the uninfected mice [35](Supplementary Fig. S6a).

We next analyzed the cytokine gene expression in the adipose tissue of HFD mice at 8 and 20 wk. p.i. *Ccl5* and *Il1b* were expressed at significantly higher levels in *M. tuberculosis*-infected HFD mice compared to uninfected HFD controls at 20 wk. p.i. (Fig. 5b) while only *Cxcl1* as slightly increased at 8 wk. p.i. (Supplementary Fig. S6b). In general, HFD mice expressed higher levels of chemokines and cytokines genes compared to chow-diet mice (Fig. 5b and Supplementary Fig. S6b). Mice fed a HFD developed adipocyte hypertrophy in the absence of infection that was not further increased after 8 or 20 wk. of *M. tuberculosis* infection (Fig. 5c and Supplementary Fig. S6c). Of note, uninfected mice fed control diet had modest age-related adipocyte hypertrophy that might have negated the effect of infection. These results were matched by no further changes in the expression levels of *Lpl*, *Cd36* and *Pnpla2* in pgWAT from infected mice fed with HFD (Supplementary Fig. S6d).

Since the number of inflammatory cells in pgWAT was significantly increased after aerosol *M. tuberculosis* infection in HFD mice, we performed a GTT to check whether this additional burden of adipose tissue inflammation perturbed systemic glucose mobilization. Aerosol infection abrogated the glucose intolerance caused by HFD and reduced the area under the curve (AUC) to the level of uninfected control mice (Fig. 5d). Plasma levels of insulin (Fig. 5e) and adiponectin and leptin (Fig. 5f), adipokines that control cytokine production, appetite and body weight [25,36], were significantly lower in *M. tuberculosis*-infected HFD mice compared to uninfected HFD controls. These changes correlated with lower HDL and LDL plasma levels, body weight and decreased pgWAT and iWAT mass in HFD mice at 20 wk. p.i. (Fig. 5g-i). We confirmed that food consumption was similar in both groups of mice treated with HFD (Supplementary Fig. S6e). Since adipocyte hypertrophy was not further increased by infection in HFD mice (Fig. 5c and Supplementary Fig. S6c), *Lipe* gene expression was increased (Supplementary Fig. S6d) and the tissue mass was decreased (Fig. 5i), these findings are consistent with the hypothesis that lipolysis is increased and adipogenesis is inhibited by TB in late time points. The gene expression of some markers for adipogenesis (*Cebpa*, *Ppara*, *Pparg*, *Bmp4* and *Ebf1*) was measured and no differences were observed between uninfected mice or 20 wk. after infection when on a HFD (Supplementary Fig. S6f). Although no tissue mass or body weight loss was observed in mice on a chow diet, *Cebpa* and *Ebf1* gene expression was increased after 20 wk. of infection compared to uninfected mice, indicating an induction of adipogenesis late after infection. Taken together, our results suggest that despite exacerbating diet-induced adipose tissue inflammation, infection with *M. tuberculosis* restored glucose tolerance and insulin levels in HFD mice late after infection. Moreover, mice on a HFD have similar lung and spleen bacterial burden and lung pathology than mice on a chow diet, at 8 and 20 wk. p.i. (Supplementary Fig. S6g), even though there is indications of tissue mass loss or cachexia and increased inflammation.

3.6. Rictor expression in adipocytes is required for infection-induced adipose tissue inflammation

We next investigated the role of Akt signaling in TB-associated adipose tissue inflammation. We challenged Adiponectin-Cre;Rictor$^{fl/fl}$ mice that lack expression of the mTORC2 regulatory subunit *Rictor* in mature adipocytes [17] with *M. tuberculosis* for 8 wk. Adipose tissue-resident immune cell numbers were comparable in uninfected WT and Adiponectin-Cre:Rictor$^{fl/fl}$ mice but the total numbers of MΦ, IMΦ, PMN, DC and T cells were significantly lower in infected Adiponectin-Cre:Rictor$^{fl/fl}$ mice compared to the infected WT mice (Fig. 6a). While MΦ showed reduced populations of Ly6C^{-} and Ly6C^{+} cells in Adiponectin-Cre:Rictor$^{fl/fl}$ mice, only Ly6C^{-} were significantly decreased in IMΦ (Fig. 6b-c). The expression of *Ccl5* and *Tnfa* mRNA were significantly reduced in pgWAT from infected Adiponectin-Cre:Rictor$^{fl/fl}$ mice compared to the infected WT mice (Fig. 6d). The reduced immune cells and cytokine gene expression in Adiponectin-Cre:Rictor$^{fl/fl}$ infected mice was accompanied with decreased adipocyte average cell size and percentage of hypertrophied cells (area > 2500 μm^2) with a corresponding increased percentage of cells with small area (0–1200 μm^2) (Fig. 6e). However, there was only a trend for reduced lung pathology

Fig. 4. Perturbation of lipid metabolism and glucose tolerance in pgWAT tissue from mice infected with *M. tuberculosis*. (a) Gene expression of *Lpl*, *Cd36*, *Pnpla2*, and *Lipe* in perigonadal white adipose tissue (pgWAT) from uninfected mice and mice infected with *M. tuberculosis* for 8 wk. (b) Concentration of glycerol and non-esterified fatty acids (NEFA) in plasma from fasted uninfected and infected mice (8 wk. p.i.) after 15 min of PBS or insulin (0·75 U/kg) i.p. injection. (c) Protein expression of HSL and its phosphorylated form in pgWAT from uninfected mice and mice infected with *M. tuberculosis* for 8 wk. (d) Protein expression of IR and Akt and their phosphorylated forms in pgWAT from uninfected mice and mice infected with *M. tuberculosis* for 8 wk. (e) Glucose tolerance test (GTT) was performed in mice that were uninfected or infected with *M. tuberculosis* for 8 wk. and after overnight fasting. Area under curve (AUC) was calculated from the resulting graphs. (f) GTT after 20 wk. of infection. (g) Insulin and glucose concentrations in plasma from uninfected mice or infected mice for 8 and 20 wk. Data are expressed as mean ± SD (n = 6–8). The experiments were repeated at least twice. *$P < 0·05$, **$P < 0·01$ and ***$P < 0·001$. See also Supplementary Fig. S4.

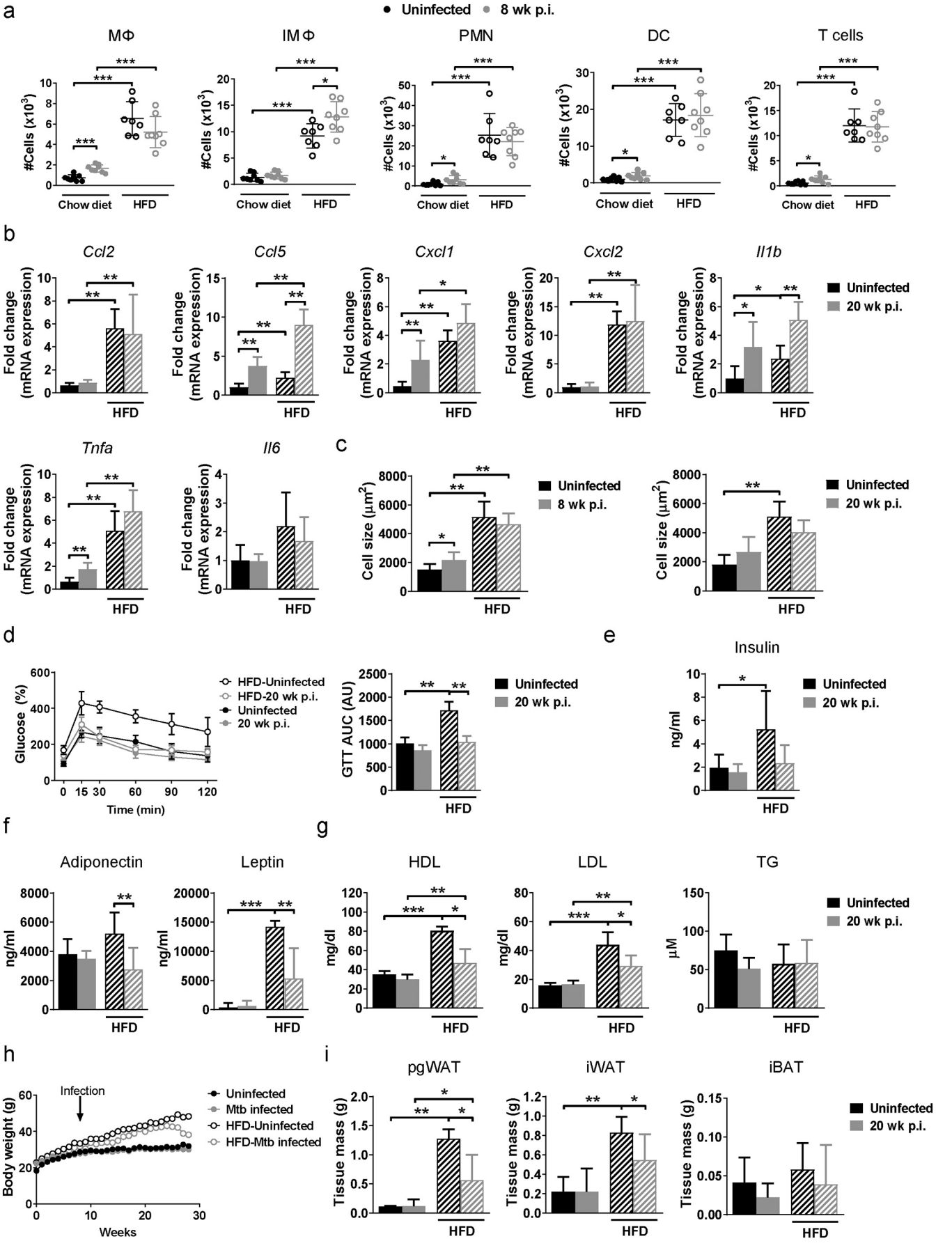
a
Uninfected
8 wk p.i.
MΦ
IMΦ
PMN
DC
T cells
#Cells (x10^3)
Chow diet
HFD
b
Ccl2
Ccl5
Cxcl1
Cxcl2
Il1b
Tnfa
Il6
Fold change (mRNA expression)
HFD
Uninfected
20 wk p.i.
c
Cell size (μm^2)
Uninfected
8 wk p.i.
20 wk p.i.
d
Glucose (%)
HFD-Uninfected
HFD-20 wk p.i.
Uninfected
20 wk p.i.
Time (min)
GTT AUC (AU)
e
Insulin
ng/ml
f
Adiponectin
Leptin
g
HDL
LDL
TG
mg/dl
μM
h
Infection
Body weight (g)
Uninfected
Mtb infected
HFD-Uninfected
HFD-Mtb infected
Weeks
i
pgWAT
iWAT
iBAT
Tissue mass (g)

and bacterial load in infected Adiponectin-Cre:Rictor$^{fl/fl}$ mice compared to the infected WT mice that was not statistically significant (Fig. 6f).

As an alternative approach to test the role of Akt in TB-associated adipose tissue inflammation we used the anti-diabetic drug metformin. Although it was reported that metformin reduces Akt phosphorylation on S473 [37], there is controversy on its mechanism of action in Akt signaling [38]. Wild type mice were infected with *M. tuberculosis* and then treated with metformin beginning 1 wk. p.i. Metformin treatment was associated with a reduced percentage of CD11b^{+} cells (Fig. 6g) and hypertrophic adipocytes in pgWAT as compared to untreated infected mice (Fig. 6h). Altogether, these results indicate that Akt signaling regulated by mTORC2 in adipocytes is implicated in the adipose tissue inflammation and the associated adipocyte hypertrophy that develop in *M. tuberculosis*-infected mice. The data further imply that mTORC2 is activated following aerosol infection with *M. tuberculosis* and that it subsequently triggers changes in the regulation of glucose and lipid metabolism.

4. Discussion

In the present study, we describe an inflammatory response in diverse adipose tissues following aerosol *M. tuberculosis* infection in mice. In contrast to the phenomenon of metaflammation described in models of diet-induced obesity, adipose tissue inflammation in the context of TB was not associated with insulin resistance or glucose intolerance. Aerosol TB challenge led to Akt pathway activation in adipocytes, increasing the response to insulin and promoting adipocyte hypertrophy. We further showed that adipose tissue inflammation depended on adipocyte intrinsic signaling pathways. In vitro infection with *M. tuberculosis* induced cytokine expression by differentiated adipocytes while adipose tissue inflammation in vivo required TLR2/4 expression in non-hematopoietic cells and the mTORC2 subunit Rictor specifically in mature adipocytes.

Adipose tissue inflammation is an early feature in the progression from non-diabetic obesity to insulin resistance and T2D. One model [21,27] holds that with high fat intake, elevated NEFA, activate adipose tissue resident macrophages and adipocytes through TLR2/4 and trigger chemokine release by both immune cells and adipocytes. At the same time, adipocytes respond to cytokines generated locally with altered lipid metabolism, becoming hypertrophic and releasing NEFA and glycerol that can drive lipid accumulation in liver and skeletal muscle. The result of these processes is activation of several kinases (JNK, IKK and PRK) in adipocytes that block IR signaling, leading to systemic glucose intolerance and insulin resistance. Adipose tissue inflammation can also result from activation of tissue-resident NK cells responding to cell stress and death of hypertrophied adipocytes [24,25]. Signals generated by activated NK cells promote leukocyte recruitment to the tissue and proliferation and polarization of macrophages. A third model proposes a different timing of the events whereby adipocyte insulin resistance initiates macrophage recruitment via PI3K signaling [39]. None of these models explains the adipose tissue inflammation and the adipocyte increased insulin sensitivity we observed in mice following aerosol infection with *M. tuberculosis*.

In our study, aerosol infection of C57BL/6J mice with 50 CFU of virulent *M. tuberculosis* Erdman promoted leukocyte accumulation in pgWAT by 4 wk. Adipocyte hypertrophy and cell stress are implicated in promoting metaflammation, but in our aerosol TB experiments adipose tissue inflammation developed before adipocyte hypertrophy was evident. The liver is a well described site for *M. tuberculosis* dissemination following aerosol challenge, so it was unsurprising that we observed liver inflammation at 4 and 8 wk. p.i. In contrast, we were unable to detect *M. tuberculosis* in pgWAT by culture, microscopy, or PCR for bacterial gDNA. A prior study recovered 0.1–0.9 $\log_{10}$ CFU in pgWAT from 4 out of 6 mice infected by aerosol with 200 CFU of *M. tuberculosis* H37Rv while no bacteria were found in pgWAT of mice infected with 50 CFU [12]. Other routes of administration, intravenously at 8×10^4 CFU and intranasal at 320 CFU, also showed presence of bacteria in the visceral and subcutaneous adipose tissues [10,11]. In vitro experiments have shown that *M. tuberculosis* can infect and persist in a non-replicating state in cultured human adipocytes [9]. Furthermore, *M. tuberculosis* genomic DNA was identified in adipose tissue samples from a minority of human TB patients [9]. It is possible that an extremely small number of bacilli might have been present in the adipose tissues from our experiments, but it is very unlikely that viable bacilli were present in enough numbers to generate a progressive inflammatory response of the magnitude we observed in mice with TB. We speculate that other signals, perhaps from systemic cytokines or *M. tuberculosis* components conveyed in mycobacterial vesicles and/or pro-inflammatory exosomes [26,40] could mediate lung-adipose tissue crosstalk via TLR2/4 activation. Adipocytes express TLR2 and TLR4 on the outer cell membrane that are activated by fatty acids and induce an inflammatory response in both adipocytes and surrounding adipose tissue resident macrophages by activating kinases, including JNK, IKK, and PKR [27,30,41]. Interestingly, these same pathways are activated in innate immune cells by *M. tuberculosis*, leading us to hypothesize that bacteria might act on adipocytes and/or adipose tissue macrophages and modulate the metabolic function of the organ. Our finding that adipose tissue inflammation depended on TLR2/4 expression in non-hematopoietic cells (presumably adipocytes) in the absence of detectable bacilli supports this model.

Adipose tissue inflammation in *M. tuberculosis*-infected mice was associated with increased adipocytes cell size and systemic glucose tolerance, along with Akt activation and decreased glycerol and NEFA plasma levels. The observed glucose tolerance might be due in part to increased glucose utilization following a shift to glycolytic metabolism in activated leukocytes responding to infection [42,43]. The attenuated form of *M. bovis*, the bacillus Calmette-Guerin (BCG) vaccine, has also been related with a switch of the immune cells from oxidative phosphorylation to aerobic glycolysis in T1D [44]. Three years after BCG treatment, T1D patients had lower levels of HbA1c that was attributed to increased glucose consumption. However, the lack of changes in insulin sensitivity in *M. tuberculosis*-infected mice indicates that adipose tissue inflammation is not invariably associated with insulin resistance. In that regard, proinflammatory signaling in adipocytes was reported to promote adipose tissue remodeling and expansion while its inhibition lead to ectopic lipid accumulation and glucose intolerance [45]. As expected, mice fed with HFD developed adipose tissue inflammation in the absence of infection that was further exacerbated by *M. tuberculosis* infection at the 8 wk. time point. The observed reduction of pgWAT mass in HFD late after infection

Fig. 5. *M. tuberculosis* infection exacerbates adipose tissue inflammation in mice on HFD. (a) Number of macrophages (MΦ), inflammatory macrophages (IMΦ), polymorphonuclear cells (PMN), dendritic cells (DC) and T cells in perigonadal white adipose tissue (pgWAT) from uninfected mice or mice infected for 8 wk. and were fed chow or HFD 8 wk. before infection. (b) Gene expression of *Ccl2*, *Ccl5*, *Cxcl1*, *Cxcl2*, *Il1b*, *Tnf1*, and *Il6* in pgWAT from uninfected mice or mice infected for 20 wk. (c) Adipocyte area in pgWAT from uninfected mice and mice infected for 8 or 20 wk. (d) Glucose tolerance test (GTT) in uninfected mice and mice that were infected for 20 wk. untreated or treated with HFD. (e) Plasma concentration of insulin in uninfected mice and mice that were infected for 20 wk. (f) Plasma concentrations of adiponectin and leptin in uninfected mice and mice that were infected for 20 wk. (g) Concentration of HDL, LDL and TG in plasma from uninfected mice and mice that were infected for 20 wk. (h) Body weight from uninfected or infected mice that were on a chow or HFD. (i) pgWAT, inguinal white adipose tissue (iWAT), interscapular brown adipose tissue (iBAT) mass in uninfected mice or mice that were infected for 20 wk. on a chow or HFD. Data are expressed as mean ± SD (n = 6–8). All the experiments were repeated at least twice. *P < 0·05, **P < 0·01 and ***P < 0·001. See also Supplementary Figs. S5 and S6.

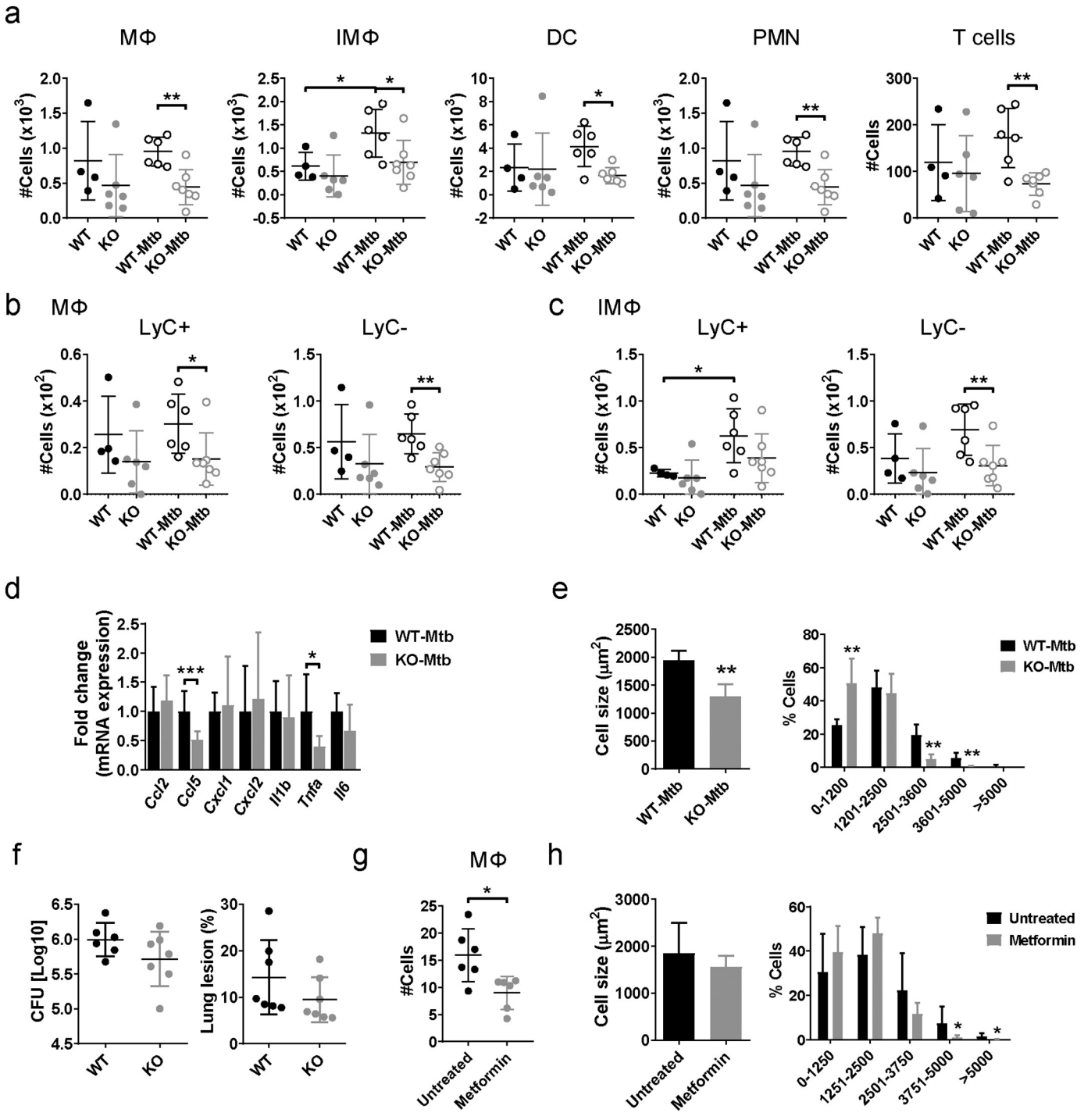

Fig. 6. mTORC2/Akt activation is required for the *M. tuberculosis*-induced adipose tissue inflammation. (a) Number of macrophages (MΦ), inflammatory macrophages (IMΦ), dendritic cells (DC), polymorphonuclear cells (PMN), and T cells in perigonadal white adipose tissue (pgWAT) in adiponectin-Cre;Rictor$^{fl/fl}$ mice that were infected or not with *M. tuberculosis* for 8 wk. (b) Number of Ly6C^{-} and Ly6C^{+} populations in MΦ from pgWAT. (c) Number of Ly6C^{-} and Ly6C^{+} populations in IMΦ from pgWAT. (d) Gene expression of *Ccl2*, *Ccl5*, *Cxcl1*, *Cxcl2*, *Il1b*, *Tnf1*, and *Il6* in pgWAT. (e) Mean of adipocyte area size and percentage of cells distributed in different bins regarding their area from pgWAT. (f) Lung bacterial load (left panel) and lung inflammation expressed as % of total lung area examined (right panel) in WT and adiponectin-Cre;Rictor$^{fl/fl}$ mice 8 wk. p.i. (g) C57BL/6J mice were treated with metformin (1·83 mg/ml in water ad libitum) 1 wk. after infection and tissues were harvested 5 wk. p.i. (h) Number of MΦ in pgWAT. (i) Mean of adipocyte area size and percentage of adipocytes distributed in different bins regarding the cell area from pgWAT from untreated or metformin treated infected mice. All the experiments were repeated at least twice. $^{*}P < 0{\cdot}05$, $^{**}P < 0{\cdot}01$ and $^{***}P < 0{\cdot}001$.

points to a shift in the lipid metabolism with a defect in lipid storage and adipogenesis failing to generate new adipocytes to restore the dead cells in the tissue. Since mice on a HFD have an increased tissue mass before infection, they could be more protected to the infection. Although we have not seen any difference in bacterial burden or pathology in obese vs lean mice, epidemiological and clinical studies have identified an association of high body mass index with protection against progression from latent TB infection to active TB disease and for reduced TB disease severity and better outcomes [46,47]. Whether that reflects an energy reserve to fuel immunity against chronic infection, or the direct participation of adipose tissue in host defense is unresolved. Some epidemiological and clinical studies

have shown that plasma lipid levels vary during the progression of the disease in TB patients [48] and we believe this could be associated to an adaptation of the host to infection, or an alteration of host lipid metabolism by the pathogen to persist within the host. It remains unresolved whether the adipose tissue and metabolic events we observed following *M. tuberculosis* challenge serve to prolong the well-being of the host, or represent a collateral effect of the infection, or if this is a mechanism whereby *M. tuberculosis* modulates glucose and lipid metabolism to impair host adaptation of the metabolic demands of immunity to chronic infection.

In summary, we report that adipose tissue inflammation and adipocyte hypertrophy developing in the context of TB disease appears to be qualitatively different from metaflammation, with no tendency to promote metabolic syndrome. Regardless of the consequences for glucose metabolism, *M. tuberculosis*-mediated increased inflammation in adipose tissue reflects a novel requirement for Rictor expression and mTORC2 signaling in adipocytes and is not a passive effect of increased leukocyte infiltration of fat. Whether this signaling network between the lung and adipose tissue ultimately benefits the host or the pathogen remains to be determined, pathogen seems to create a biphasic phenomenon where initially prepares the host for survival and at late stages shifts the lipid metabolism towards tissue mass loss and cachexia. Emerging evidence for a protective effect of metformin in TB suggests that the perturbation of adipocyte signaling and lipid metabolism identified in our studies may be detrimental for the host and may also be a target for therapeutic intervention.

Supplementary data to this article can be found online at https://doi.org/10.1016/j.ebiom.2019.06.052.

Acknowledgements

We thank the FACS Core, Animal Medicine Core and the Morphology Core at UMMS and Dr. Christina Bauer, director of the Sanderson Center for Optical Experimentation at UMMS. We would also like to thank Dr. Christopher Sassetti for supplying the YFP-expressing *M. tuberculosis* Erdman and Kelly Cavallo for assisting with staining and imaging of adipocytes.

Funding sources

This work was funded by the NIH grant HL018849 (to H.K.), R01DK094004 (to D.G.), Immunomonitoring platform grant #IAF311006 (to M.P.), A*STAR JCO-CDA grant 15302FG151 and Singapore Immunology Network core fund (to A.S.).

Declaration of interest

A.S. has filed a patent with respect to the use of metformin for controlling Mycobacterial infections (US 9539222). Other authors declare no competing interest.

Author contributions

N.M. designed and performed the experiments, collected and interpreted the data and drafted the manuscript, C.Y.C., M.P. and J.L performed the RNAseq experiment, analyzed and interpreted the data. A.C. and K.W. helped performing the experiments. N.K., A.S., Y.T. and D.A.G. gave suggestions to the experiments design and interpreted the data. H.K. designed the experiments, interpreted the data and drafted the manuscript. All authors reviewed the manuscript.

References

[1] World Health Organization. Tuberculosis: fact sheets. https://www.who.int/en/news-room/fact-sheets/detail/tuberculosis; 2019. [Reviewed Nov 2018].
[2] Gagneux S. Host-pathogen coevolution in human tuberculosis. Philos Trans R Soc Lond B Biol Sci 2012;367(1590):850–9.
[3] Tiemersma EW, van der Werf MJ, Borgdorff MW, Williams BG, Nagelkerke NJ. Natural history of tuberculosis: duration and fatality of untreated pulmonary tuberculosis in HIV negative patients: a systematic review. PloS one 2011;6(4):e17601.
[4] Stanley SA, Cox JS. Host-pathogen interactions during *Mycobacterium tuberculosis* infections. Curr Top Microbiol Immunol 2013;374:211–41.
[5] Cadena AM, Flynn JL, Fortune SM. The importance of first impressions: early events in *Mycobacterium tuberculosis* infection influence outcome. MBio 2016;7(2):e00342–416.
[6] Cooper AM. Cell-mediated immune responses in tuberculosis. Annu Rev Immunol 2009;27:393–422.
[7] Hickey AJ, Gounder L, Moosa MY, Drain PK. A systematic review of hepatic tuberculosis with considerations in human immunodeficiency virus co-infection. BMC Infect Dis 2015;15:209.
[8] Wang Y, Tang XY, Yuan J, Wu SQ, Chen G, Zhang MM, et al. Bone marrow granulomas in a high tuberculosis prevalence setting: a clinicopathological study of 110 cases. Medicine (Baltimore) 2018;97(4):e9726.
[9] Neyrolles O, Hernandez-Pando R, Pietri-Rouxel F, Fornes P, Tailleux L, Barrios Payan JA, et al. Is adipose tissue a place for *Mycobacterium tuberculosis* persistence? PLoS One 2006;1:e43.
[10] Agarwal P, Khan SR, Verma SC, Beg M, Singh K, Mitra K, et al. *Mycobacterium tuberculosis* persistence in various adipose depots of infected mice and the effect of antitubercular therapy. Microbes Infect 2014;16(7):571–80.
[11] Agarwal P, Pandey P, Sarkar J, Krishnan MY. *Mycobacterium tuberculosis* can gain access to adipose depots of mice infected via the intra-nasal route and to lungs of mice with an infected subcutaneous fat implant. Microb Pathog 2016;93:32–7.
[12] Beigier-Bompadre M, Montagna GN, Kuhl AA, Lozza L, Weiner 3rd J, Kupz A, et al. *Mycobacterium tuberculosis* infection modulates adipose tissue biology. PLoS Pathog 2017;13(10):e1006676.
[13] Samuel VT, Shulman GI. The pathogenesis of insulin resistance: integrating signaling pathways and substrate flux. J Clin Invest 2016;126(1):12–22.
[14] Agusti A, Barbera JA, Wouters EF, Peinado VI, Jeffery PK. Lungs, bone marrow, and adipose tissue. A network approach to the pathobiology of chronic obstructive pulmonary disease. Am J Respir Crit Care Med 2013;188(12):1396–406.
[15] D'Avila H, Melo RC, Parreira GG, Werneck-Barroso E, Castro-Faria-Neto HC, Bozza PT. Mycobacterium bovis bacillus Calmette-Guerin induces TLR2-mediated formation of lipid bodies: intracellular domains for eicosanoid synthesis in vivo. J Immunol 2006;176(5):3087–97.
[16] Shi L, Salamon H, Eugenin EA, Pine R, Cooper A, Gennaro ML. Infection with *Mycobacterium tuberculosis* induces the Warburg effect in mouse lungs. Sci Rep 2015;5:18176.
[17] Tang Y, Wallace M, Sanchez-Gurmaches J, Hsiao WY, Li H, Lee PL, et al. Adipose tissue mTORC2 regulates ChREBP-driven de novo lipogenesis and hepatic glucose metabolism. Nat Commun 2016;7:11365.
[18] Munoz-Elias EJ, Timm J, Botha T, Chan WT, Gomez JE, McKinney JD. Replication dynamics of *Mycobacterium tuberculosis* in chronically infected mice. Infect Immun 2005;73(1):546–51.
[19] Picelli S, Faridani OR, Bjorklund AK, Winberg G, Sagasser S, Sandberg R. Full-length RNA-seq from single cells using smart-seq2. Nat Protoc 2014;9(1):171–81.
[20] Robinson MD, McCarthy DJ, Smyth GK. edgeR: a bioconductor package for differential expression analysis of digital gene expression data. Bioinformatics 2010;26(1):139–40.
[21] Johnson AM, Olefsky JM. The origins and drivers of insulin resistance. Cell 2013;152(4):673–84.
[22] Gordon S, Taylor PR. Monocyte and macrophage heterogeneity. Nat Rev Immunol 2005;5(12):953–64.
[23] Ingersoll MA, Spanbroek R, Lottaz C, Gautier EL, Frankenberger M, Hoffmann R, et al. Comparison of gene expression profiles between human and mouse monocyte subsets. Blood 2010;115(3):e10–9.
[24] Lee BC, Kim MS, Pae M, Yamamoto Y, Eberle D, Shimada T, et al. Adipose natural killer cells regulate adipose tissue macrophages to promote insulin resistance in obesity. Cell Metab 2016;23(4):685–98.
[25] Wensveen FM, Jelencic V, Valentic S, Sestan M, Wensveen TT, Theurich S, et al. NK cells link obesity-induced adipose stress to inflammation and insulin resistance. Nat Immunol 2015;16(4):376–85.
[26] Prados-Rosales R, Baena A, Martinez LR, Luque-Garcia J, Kalscheuer R, Veeraraghavan U, et al. Mycobacteria release active membrane vesicles that modulate immune responses in a TLR2-dependent manner in mice. J Clin Invest 2011;121(4):1471–83.
[27] Gregor MF, Hotamisligil GS. Inflammatory mechanisms in obesity. Annu Rev Immunol 2011;29:415–45.
[28] Morris DL, Cho KW, Delproposto JL, Oatmen KE, Geletka LM, Martinez-Santibanez G, et al. Adipose tissue macrophages function as antigen-presenting cells and regulate adipose tissue CD4+ T cells in mice. Diabetes 2013;62(8):2762–72.
[29] Deng T, Lyon CJ, Minze LJ, Lin J, Zou J, Liu JZ, et al. Class II major histocompatibility complex plays an essential role in obesity-induced adipose inflammation. Cell Metab 2013;17(3):411–22.
[30] Hotamisligil GS. Inflammation, metaflammation and immunometabolic disorders. Nature 2017;542(7640):177–85.
[31] Alkhouri N, Gornicka A, Berk MP, Thapaliya S, Dixon LJ, Kashyap S, et al. Adipocyte apoptosis, a link between obesity, insulin resistance, and hepatic steatosis. J Biol Chem 2010;285(5):3428–38.
[32] Gonzales AM, Orlando RA. Role of adipocyte-derived lipoprotein lipase in adipocyte hypertrophy. Nutr Metab (Lond) 2007;4:22.
[33] Vroegrijk IO, van Klinken JB, van Diepen JA, van den Berg SA, Febbraio M, Steinbusch LK, et al. CD36 is important for adipocyte recruitment and affects lipolysis. Obesity (Silver Spring) 2013;21(10):2037–45.

[34] Sarbassov DD, Guertin DA, Ali SM, Sabatini DM. Phosphorylation and regulation of Akt/PKB by the rictor-mTOR complex. Science 2005;307(5712):1098–101.
[35] Mau T, Yung R. Adipose tissue inflammation in aging. Exp Gerontol 2018;105:27–31.
[36] Schaffler A, Scholmerich J. Innate immunity and adipose tissue biology. Trends Immunol 2010;31(6):228–35.
[37] Zakikhani M, Blouin MJ, Piura E, Pollak MN. Metformin and rapamycin have distinct effects on the AKT pathway and proliferation in breast cancer cells. Breast Cancer Res Treat 2010;123(1):271–9.
[38] Nozhat Z, Mohammadi-Yeganeh S, Azizi F, Zarkesh M, Hedayati M. Effects of metformin on the PI3K/AKT/FOXO1 pathway in anaplastic thyroid Cancer cell lines. Daru 2018;26(2):93–103.
[39] McCurdy CE, Klemm DJ. Adipose tissue insulin sensitivity and macrophage recruitment: does PI3K pick the pathway? Adipocyte 2013;2(3):135–42.
[40] Singh PP, LeMaire C, Tan JC, Zeng E, Schorey JS. Exosomes released from *M. tuberculosis* infected cells can suppress IFN-gamma mediated activation of naive macrophages. PLoS One 2011;6(4):e18564.
[41] Nguyen MT, Favelyukis S, Nguyen AK, Reichart D, Scott PA, Jenn A, et al. A subpopulation of macrophages infiltrates hypertrophic adipose tissue and is activated by free fatty acids via Toll-like receptors 2 and 4 and JNK-dependent pathways. J Biol Chem 2007;282(48):35279–92.
[42] Pearce EL, Pearce EJ. Metabolic pathways in immune cell activation and quiescence. Immunity 2013;38(4):633–43.
[43] van der Windt GJ, Pearce EL. Metabolic switching and fuel choice during T-cell differentiation and memory development. Immunol Rev 2012;249(1):27–42.
[44] Kuhtreiber WM, Tran L, Kim T, Dybala M, Nguyen B, Plager S, et al. Long-term reduction in hyperglycemia in advanced type 1 diabetes: the value of induced aerobic glycolysis with BCG vaccinations. NPJ Vaccines 2018;3:23.
[45] Wernstedt Asterholm I, Tao C, Morley TS, Wang QA, Delgado-Lopez F, Wang ZV, et al. Adipocyte inflammation is essential for healthy adipose tissue expansion and remodeling. Cell Metab 2014;20(1):103–18.
[46] Anuradha R, Munisankar S, Bhootra Y, Dolla C, Kumaran P, Babu S. High body mass index is associated with heightened systemic and mycobacterial antigen - specific pro-inflammatory cytokines in latent tuberculosis. Tuberculosis (Edinb) 2016;101:56–61.
[47] Lin HH, Wu CY, Wang CH, Fu H, Lonnroth K, Chang YC, et al. Association of obesity, diabetes, and risk of tuberculosis: two population-based cohorts. Clin Infect Dis 2018;66(5):699–705.
[48] Kornfeld H, West K, Kane K, Kumpatla S, Zacharias RR, Martinez-Balzano C, et al. High prevalence and heterogeneity of diabetes in patients with TB in South India: a report from the effects of diabetes on tuberculosis severity (EDOTS) study. Chest 2016;149(6):1501–8.